Title

Measuring full-range soil hydraulic properties for the prediction of crop water availability using gamma-ray attenuation and inverse modeling

Authors

Pinheiro, Everton Alves Rodrigues
van Lier, Quirijn de Jong
Inforsato, Leonardo
et al.

Publication Date

2019-05-01

DOI

10.1016/j.agwat.2019.01.029

Peer reviewed

Agricultural Water Management 216 (2019) 294–305

Contents lists available at ScienceDirect

Agricultural Water Management

journal homepage: www.elsevier.com/locate/agwat

Measuring full-range soil hydraulic properties for the prediction of crop water availability using gamma-ray attenuation and inverse modeling

Everton Alves Rodrigues Pinheiro[a,b,*], Quirijn de Jong van Lier[a], Leonardo Inforsato[a], Jirka Šimůnek[b]

[a] CENA/University of São Paulo, P.O. Box 96, 13416-900, Piracicaba, SP, Brazil
[b] Department of Environmental Sciences, Univ. of California, Riverside, CA, 92521, USA

ARTICLE INFO

Keywords:
Evaporation experiment
Parameter optimization
Soil hydraulic conductivity
Root water uptake

ABSTRACT

Accurate knowledge of soil hydraulic properties (*K-θ-h*) for the entire range of crop available water is essential for the prediction of soil water movement and related processes by mechanistic models, including the partitioning of surface energy fluxes into transpiration and evaporation and the dynamics of root water uptake, mandatory processes for adjustments of crop water use efficiency. We implemented an experimental and numerical protocol to obtain *K-θ-h* of eleven soils with a broad spectrum of texture and land use. Measurements of the soil water content during evaporation experiments using gamma-ray beam attenuation, a non-invasive technique, were adopted as an alternative approach to conventional measurements of the soil water pressure head. Inverse parameter optimization was performed using Hydrus-1D. The optimized *K-θ-h* functions were interpreted with respect to crop available water, where results calculated by a proposed "dynamic" method were compared with those determined using the conventional "static" criteria with standardized pressure heads. The evaporation experiment protocol allowed the determination of the *K-θ-h* relationships by inverse modeling from near-saturation to the dry range (~ -150 m) with satisfactory accuracy. Soil water retention curves of the fine-textured soils determined by the conventional method (pressure plates) deviated from those estimated by the inverse optimization near saturation and in the dry range, with the conventional method predicting larger water content values. In terms of crop available water, the "dynamic" method allowed incorporating system characteristics (atmospheric demand and crop properties) and *K-θ-h* in a process-based way, contrarily to the "static" method. Considering a specific scenario, for the fine-textured soils the "static" and "dynamic" approaches performed similarly, however, for the coarse-textured soils, they diverged significantly. No tendency could be revealed for crop water availability under different land uses, and, in general, crop available water for soils under forest use was very similar to their counterparts under agricultural use.

1. Introduction

Soil water is a key element in partitioning of surface energy fluxes into plant transpiration and soil evaporation (Vogel et al., 2017). It controls the global net biomass productivity and couples energy and biogeochemical budgets by the establishment and maintenance of natural and agricultural ecosystems (Wang et al., 2012; Pinheiro et al., 2018; Minasny and McBratney, 2018). Soil water availability to crops can be estimated using simple empirical formulations based on the upper and lower limits of available soil water, commonly defined solely on pressure head values, and thus relegating the dynamic process of soil water flow in the unsaturated zone. On the other hand, the same empirical formulations can acquire an increased physical meaning if their pressure head threshold values are calculated taking into consideration properties and variables that control the root water uptake process (e.g., the hydraulic conductivity and hydraulic conductivity gradients, together with the spatial root distribution and the atmospheric energy demand). Alternatively, robust simulations of soil water availability while dynamically linking soil-plant-atmosphere processes by the implementation of state-of-the-art vadose zone hydrology models such as Hydrus-1D (Šimůnek et al., 2016) and SWAP (Kroes et al., 2017) are highly desired. In either way, both approaches are dependent on the accurate assessment of soil hydraulic properties (*SHP*).

The traditional method to obtain soil water retention properties is based on establishing a hydrostatic equilibrium between a soil sample and a porous medium such as a filter paper, fine sand, or a porous

* Corresponding author at: CENA/University of São Paulo, P.O. Box 96, 13416-900, Piracicaba, SP, Brazil.
E-mail addresses: pinheiroear@usp.br (E.A.R. Pinheiro), qdjvlier@usp.br (Q. de Jong van Lier), inforsato@usp.br (L. Inforsato), jsimunek@ucr.edu (J. Šimůnek).

https://doi.org/10.1016/j.agwat.2019.01.029
Received 8 August 2018; Received in revised form 30 January 2019; Accepted 30 January 2019

ceramic, at a certain pressure head. In soil physics labs around the world, various equipment such as sand boxes, tension tables, and pressure plates are commonly used to subject an initially saturated soil sample to a series of gradually decreasing pressure heads (Cresswell et al., 2008; Bittelli and Flury, 2009). The obtained data pairs $\theta(h)$ of pressure heads, h, and soil water contents, θ, are then fitted using some selected analytical model of the soil-water retention function (e.g., Brooks and Corey, 1964; Campbell, 1974; van Genuchten, 1980; Durner, 1994; Groenevelt and Grant, 2004). Although this method does not provide any information about the unsaturated soil hydraulic conductivity, $K(\theta)$, a common practice in many vadose zone hydrological studies is to adopt the Mualem (1976) capillary bundle model together with independent measurements of the saturated hydraulic conductivity, K_s, and assign a pore connectivity value (λ) of 0.5 as found by Mualem (1976). However, this practice subjects simulations of soil hydrology-related processes to large uncertainties (Schaap and Leij, 2000; Vereecken et al., 2010), especially in the dry and wet ranges of soils with regular and hierarchical pore geometry, respectively.

Models that deal with root water uptake in a detailed manner by numerically solving the Richards equation with a root water uptake sink term are highly dependent on unsaturated hydraulic conductivity functions in the dry range (Javaux et al., 2008; de Jong van Lier et al., 2008, 2015; Cai et al., 2018) and require special attention to soil hydraulic parameterization. One way to reduce the uncertainty caused by the determination of *SHP* is to assess soil water retention and unsaturated hydraulic conductivity simultaneously. A well-established method to do so is to use the inverse parameter estimation of transient water flow experiments (e.g., Šimůnek et al., 1998; Peters et al., 2015). The evaporation method is one of the most popular transient flow experiments. Several modifications of this method have been proposed (e.g., Wind, 1968; Schindler, 1980; Wendroth et al., 1993; Šimůnek et al., 1998; Durner and Iden, 2011) since its introduction by Gardner and Miklich (1962). In general, the laboratory evaporation method uses tensiometers that are inserted horizontally or vertically in a soil core that is placed on a balance. While tensiometers are used to measure temporal variations of the pressure head in the soil core, a balance is used to determine temporal variations of the actual evaporation rate. The method is usually limited by the operation range of tensiometers (commonly $h > -10$ m). Another drawback besides the narrow operation range are constrained measurements in a thin soil layer around tensiometer ceramic cups, which are relatively large compared to the small soil sample. The contact between sensors and soil may also be limited, especially in soils that shrink and swell due to a high clay content or organic matter.

Measurements of the soil water content during evaporation experiments using gamma-ray beam attenuation, a non-invasive technique with high spatial resolution and allowing the use of the same soil samples throughout the entire process (Luo and Wells, 1992; Oliveira et al., 1998; Pires et al., 2005; Lobsey and Rossel, 2016), can represent an alternative approach to conventional measurements of the soil water pressure head. The main objectives of this study thus are a) to investigate this alternative method for the determination of *SHP* in soil samples, b) to interpret the resulting *SHP* with respect to crop water availability, and c) to compare crop water availability obtained using a proposed "dynamic" method with that determined using the conventional criteria of "static" pressure head values that define field capacity (FC) and the wilting point (WP).

2. Material and methods

2.1. Sampling sites

Eleven sampling sites under several land use types and covering a broad spectrum of soil textures typical of a subtropical humid climate zone (Köppen Cwa) in the southeast of Brazil were selected for this study (Fig. 1 and Table 1). Sampling sites can be grouped together according to location where each group of sites (1,2), (3,4), (5,6), (7,8), and (9,10,11) represents different land uses on nearby and similar soils. Five undisturbed soil cores (stainless steel cylinders with a height of 7 cm and an internal diameter of 7.4 cm) were collected from two depths (between 0 and 0.15 m and between 0.3 and 0.45 m) at each site. The middle point of the cylinder length corresponds to the middle depth of each interval. These sampling depths were selected based on general root length density (RLD) observations performed by de Willigen and Van Noordwijk (1987), who showed that for the majority of crops the most relevant root zone for root water uptake occurs between the soil surface and a depth of 0.4 m.

2.2. Evaporation experiments

Evaporation experiments were carried out in the lab to determine unsaturated soil hydraulic properties of each sampled soil layer using the undisturbed samples. For each soil layer, five replicates were slowly saturated by capillarity from bottom to top using a 0.01 mol L^{-1} $CaSO_4$ solution. Once full saturation was reached, the sample bottom was sealed with plastic foil, the soil samples were weighed, and the first measurements of the soil water content were made by determining the attenuation of a collimated gamma-ray beam at five vertical positions, 10, 15, 20, 35, and 50 mm below the soil sample surface. These measurements were performed twice at each vertical position, with the sample being turned by 90° between measurements (Fig. 2).

Samples were weighed and soil water contents recorded according to this protocol each 24 h. The evaporation experiment was ceased when the weight change during a 24-h period became negligible (< 1 g d^{-1}, corresponding to an average water content reduction less than 0.0035 m^3 m^{-3} d^{-1}), which usually took about three to four weeks. At the end of the experiment, the final water content of the soil cores was determined by oven drying at 105 °C.

Gamma-ray attenuation is a well-stablished technique that can be used for measuring soil-water content. Its advantages include the applicability to the entire range of water contents and a high accuracy. As no sensor needs to be inserted inside the soil core, there is no alteration at all of the sample structure (Pires et al., 2005). Additionally, unlike many other measurement techniques, it does not require calibration for each soil.

In this study, a collimated gamma-ray source of ^{137}Cs with radioactivity of 11.1 GBq and an energy peak of 661.6 keV was used. The source was coupled with a NaI(Tl) scintillation detector (7.62 × 7.62 cm), which was attached to a photomultiplier tube. A photon counter was interfaced with a computer, which stores data automatically. Circular collimators were adjusted and aligned between a source (diameter 3 mm) and a detector (diameter 4.5 mm). More details about the used gamma-ray attenuation device can be found in Pires et al. (2005).

The soil core was positioned between the source and the detector. The gamma-photons passing through the sample were counted by the detector for 20 s and expressed as photon beam intensity I (m^{-2} s^{-1}). The volumetric soil water content, θ, was calculated using the Beer-Lambert attenuation law (Wang et al., 1975):

$$\theta = \frac{\ln\left(I_0/I\right)}{\mu_w \rho_w x} \quad (1)$$

where I_0 (m^{-2} s^{-1}) is the photon beam intensity crossing the experimental unit with oven-dry soil (corresponding to the same soil cores used during the evaporation phase); μ_w (m^2 kg^{-1}) is the mass attenuation coefficient of the water fraction for the corresponding radiation energy, ρ_w (kg m^{-3}) is the water density, and x (m) is the thickness of the soil sample.

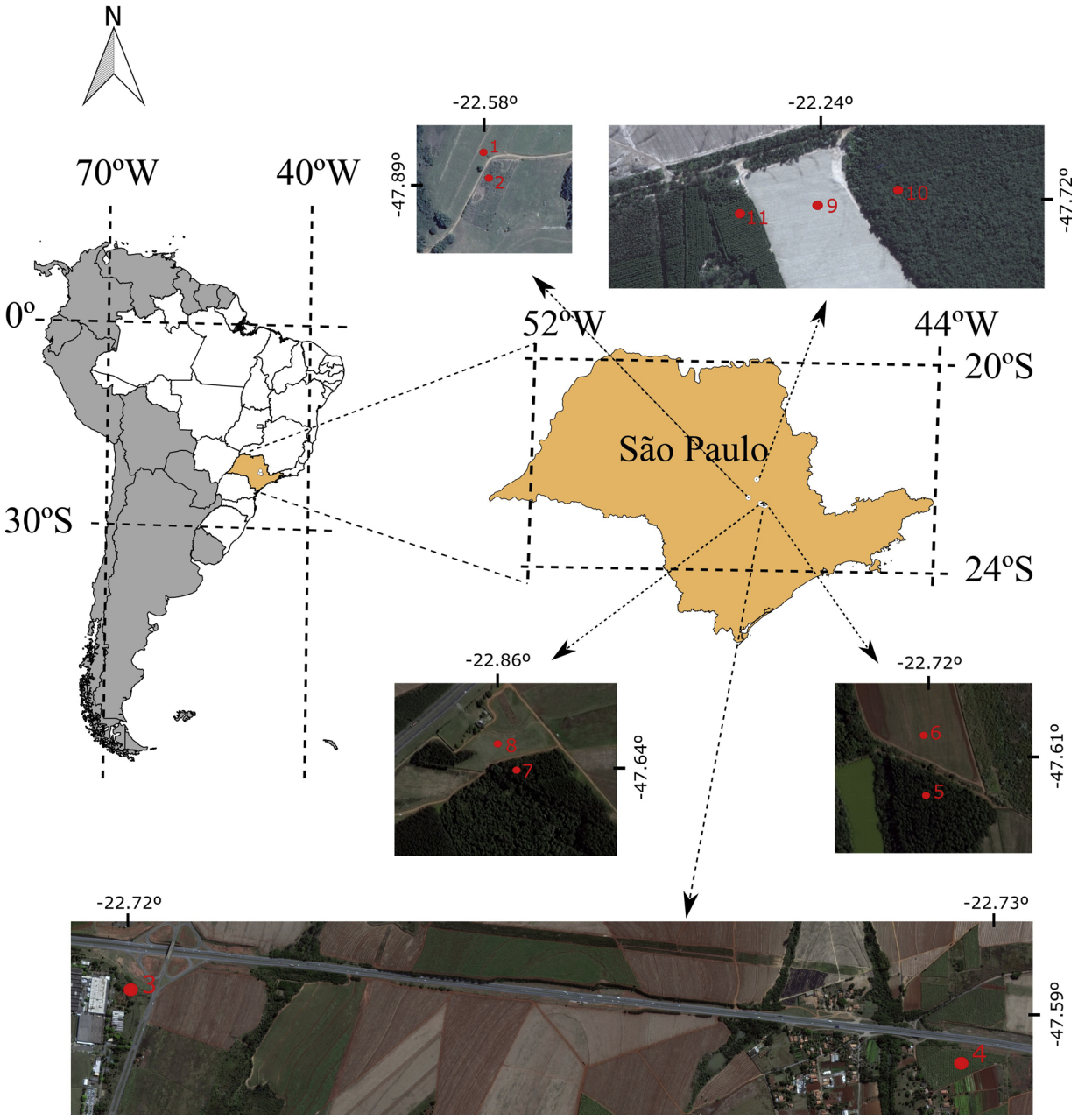

Fig. 1. Geographical locations and aerial images of the sampling sites.

2.3. Hypothetical experiments

The determination of *SHP* from a conventional evaporation experiment usually relies on pressure heads, $h(t)$, measured using tensiometers at selected positions in a soil sample. These pressure head measurements are used to define the objective function to be minimized during the inverse parameter optimization process. In our experimental setup, tensiometer readings were replaced with gamma-ray attenuation measurements, resulting in water contents rather than pressure heads. To evaluate the performance of the inverse parameter optimization process when the objective function (Φ, a sum of squared deviations between measured and simulated values) is defined in terms of soil water contents versus time, $\theta_i(t_i)$, rather than in terms of conventional pressure heads versus time $h_i(t_i)$, a hypothetical evaporation experiment was simulated using Hydrus-1D.

The sample geometry and measurement positions in the hypothetical experiment were the same as in the real experiment. Water content and pressure head measurements, $\theta_i(t_i)$ and $h_i(t_i)$, respectively, were simulated for five positions in a 7 cm high soil column and at potential evaporation rate of 0.25 cm d^{-1}. The true parameter values of soil hydraulic properties of Clay and Sandy Loam were obtained from the ROSETTA module (Schaap et al., 2001). To make the virtual dataset more realistic, a normally distributed noise with a zero mean and a standard deviation of 1 cm was superimposed on the virtual dataset $h_i(t_i)$, similarly as done by Peters and Durner (2008). The perturbed $h_i(t_i)$ values were then converted to $\theta_i(t_i)$ using the true sets of soil hydraulic parameters.

2.4. Inverse parameter optimization

Both laboratory and hypothetical soil evaporation experiments were evaluated using the Hydrus-1D software package (Šimůnek et al., 2016), which simulates one-dimensional variably-saturated water flow in porous media by numerically solving the Richards equation. Hydrus-

Table 1
Particle size distribution, soil texture class, and current land use at the 11 sampling sites.

Site	Depth m	Particle size fraction (kg kg^{-1})			Soil texture class	Land use
		Sand	Silt	Clay		
1	0.00-0.15	0.885	0.027	0.088	Loamy fine sand	Pasture
	0.30-0.45	0.856	0.031	0.113		
2	0.00-0.15	0.835	0.027	0.138	Sandy Loam	Sugarcane
	0.30-0.45	0.835	0.015	0.150		
3	0.00-0.15	0.204	0.167	0.629	Clay	Fallow
	0.30-0.45	0.221	0.125	0.654		
4	0.00-0.15	0.181	0.127	0.692	Clay	Sugarcane
	0.30-0.45	0.139	0.106	0.755		
5	0.00-0.15	0.481	0.113	0.406	Sandy clay	Native Forest
	0.30-0.45	0.509	0.061	0.430		
6	0.00-0.15	0.427	0.092	0.481	Clay	Pasture
	0.30-0.45	0.388	0.081	0.531		
7	0.00-0.15	0.233	0.076	0.691	Clay	Native Forest
	0.30-0.45	0.278	0.055	0.667		
8	0.00-0.15	0.202	0.045	0.753	Clay	Annual crops
	0.30-0.45	0.168	0.038	0.794		
9	0.00-0.15	0.856	0.031	0.113	Loamy fine sand	Sugarcane
	0.30-0.45	0.845	0.029	0.126		
10	0.00-0.15	0.847	0.039	0.114	Loamy fine sand	Native Forest
	0.30-0.45	0.850	0.024	0.126		
11	0.00-0.15	0.856	0.031	0.113	Loamy fine sand	Eucalyptus (planted forest)
	0.30-0.45	0.862	0.012	0.126		

1D additionally implements the Marquardt-Levenberg parameter estimation method for inverse optimization of soil hydraulic parameters. This method is a gradient-type minimization one, which is sensitive to the initial estimates (Abbaspour et al., 2001).

Unsaturated soil hydraulic properties were assumed to be described by the analytical *K*-*θ*-*h* functions defined by the van Genuchten-Mualem model (Mualem, 1976; van Genuchten, 1980):

$$\Theta = [1 + |\alpha h|^{n}]^{(1/n)-1} \quad (2)$$

$$K = K_s \Theta^{\lambda}[1 - (1 - \Theta^{n/(n-1)})^{1-(1/n)}]^2 \quad (3)$$

with $\Theta = (\theta - \theta_r)/(\theta_s - \theta_r)$ is the effective saturation, θ (m^3 m^{-3}) is the water content, h (m) is the pressure head, and K (m d^{-1}) is the unsaturated hydraulic conductivity. Six parameters define the *SHP*s and will be referred to as the VGM parameters: θ_r (residual water content), θ_s (saturated water content), K_s (saturated hydraulic conductivity), and shape parameters α (m^{-1}), n, and λ.

The upper and lower water flow boundary conditions were set as atmospheric and constant (zero) flux boundary conditions, respectively. In the analysis of laboratory experiments, the surface evaporation flux was calculated for each time interval from the observed mass difference over a time interval and used as a time-variable boundary condition. In the analysis of hypothetical experiments, the constant potential evaporation rate of 0.25 cm d^{-1} was used as the upper boundary flux.

Soil water contents measured at five positions versus time were included in the objective function Φ to be minimized by Hydrus-1D in the analysis of laboratory experiments. In the analysis of hypothetical

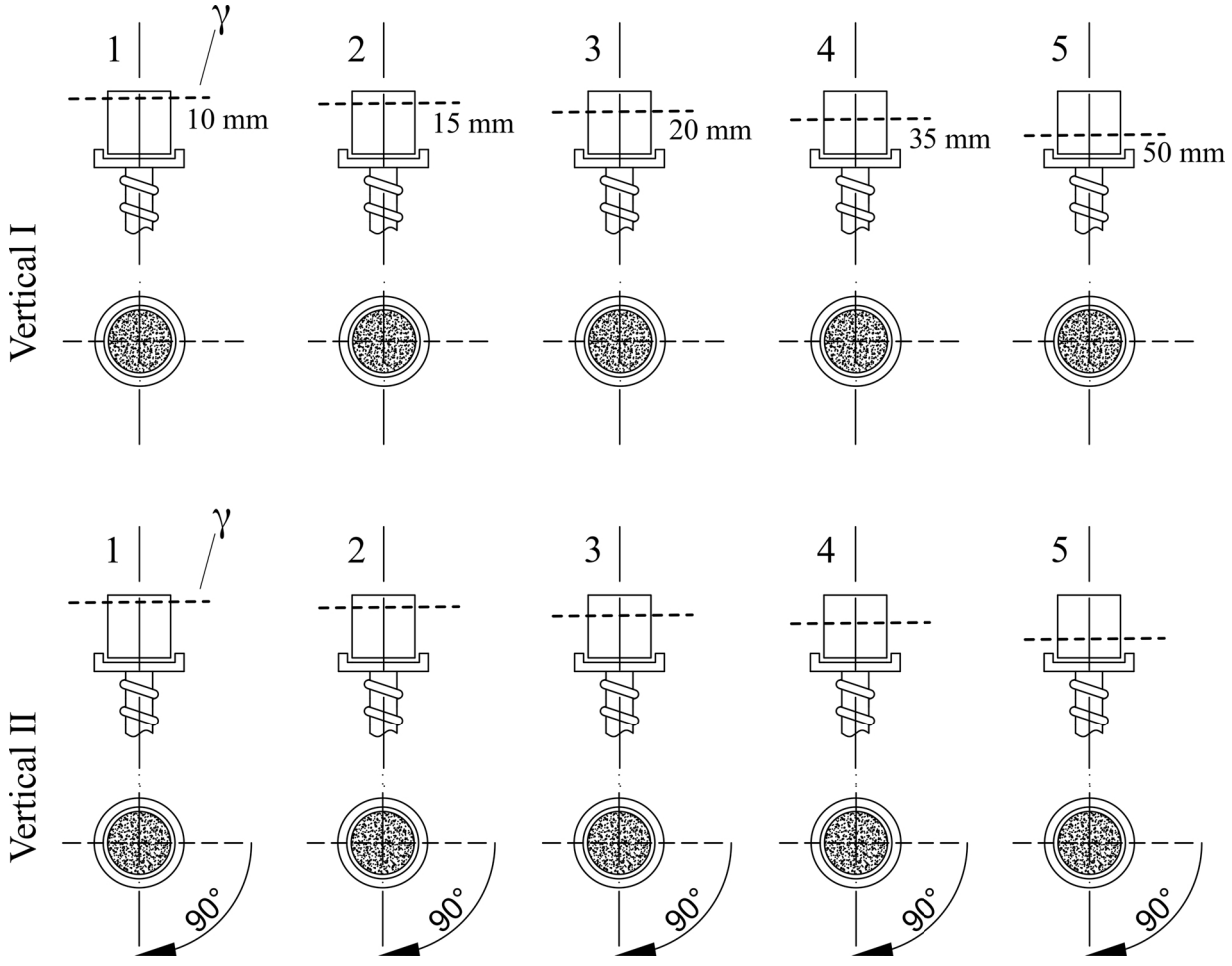

Fig. 2. Schematic illustration of the gamma attenuation measurement protocol (5 heights and 2 rotations).

experiments, the perturbed $\theta_i(t_i)$ and $h_i(t_i)$ were used separately to define the objective function Φ. In the case when Φ was defined using $h_i(t_i)$, the final total water volume in the soil sample was included in Φ as well, in order to position the retention curve along the θ axis (Šimůnek et al., 1998).

To avoid physically unrealistic estimates in the analysis of laboratory experiments, the initial set of soil hydraulic parameters was selected using the neural network module ROSETTA (Schaap et al., 2001) and the parameters optimized using data obtained from pressure plate apparatus experiments. For both soil evaporation experiments (laboratory and hypothetical), the five optimized VGM soil hydraulic parameters were: θ_s, α, n, K_s, and λ. The residual water content, θ_r, was set equal to the final measured value of the soil water content, when the soil was close to air-dry. For the laboratory experiment, a set of hydraulic parameters was estimated for each of the five replicates. To transform these five sets of parameters into a single set, the optimized VGM parameters for each replicate were used to generate 100 values of K and θ in the pressure head observation range (from -150 to -0.1 m). The resulting 500 data pairs were then processed using the RETC software (van Genuchten et al., 1991) to generate a unique hydraulic parameter set for each soil layer.

2.5. Further verification of the accuracy of the optimized soil hydraulic parameters

The mean water content values of the soil cores calculated from the sample weight change over time were compared with the simulated mean water content values for the same time intervals. The mean water content simulated by the Hydrus-1D was obtained by dividing the volume of water in the entire flow domain by the column height. The accuracy was quantified using the Nash-Sutcliffe efficiency (*NSE*) and root mean squared error (*RMSE*) coefficients:

$$NSE = 1 - \frac{\sum_{i=1}^{n}(\theta_i - \theta_i^*)^2}{\sum_{i=1}^{n}(\theta_i - \bar{\theta}_i)^2} \quad (4)$$

$$RMSE = \sqrt{\frac{1}{n}\sum_{i=1}^{n}(\theta_i - \theta_i^*)^2} \quad (5)$$

respectively, where n is the number of data points, θ_i is the measured value of the mean water content in the soil column at time t_i, $\theta_i^*$is the corresponding simulated value by the Hydrus-1D, and $\bar{\theta}_i$is the mean value of the water content over the entire experiment.

2.6. Crop water availability

The optimized soil hydraulic parameters were used to predict the total and readily available water (TAW and RAW, respectively) of the analyzed soils. The threshold values for calculating crop water availability are customarily defined as the water content at field capacity (θ_{fc}), the upper limit of TAW and RAW, the limiting water content (θ_{lim}), the lower limit of RAW, and the water content at wilting point (θ_{wp}), the lower limit of TAW. Values of θ_{fc}, θ_{lim}, and θ_{wp} are commonly calculated using fixed pressure heads. Common pressure head values used to assess field capacity h_{fc} are -3.3 m or -1.0 m, for h_{lim} are between -2.0 m and -10 m (Taylor and Ashcroft, 1972), and for h_{wp} are most commonly assumed equal to -100 m or -150 m.

The approach of determining water content values for field capacity and critical and wilting point conditions based on fixed pressure heads will be compared with their estimation using "dynamic" criteria. The water content at field capacity, θ_{fc}, can be determined by simulating a drainage experiment without plants, rainfall, and evaporation using a flux density criterion of 1 mm d^{-1} (e.g., Twarakavi et al., 2009) at the lower soil boundary (here considered at a depth of 0.6 m). The adopted criterion of the bottom flux of 1 mm d^{-1} is reasonable also for tropical soils (de Jong van Lier and Wendroth, 2016; de Jong van Lier, 2017).

The limiting water content, θ_{lim}, and the water content at wilting point, θ_{wp}, can be related to the matric flux potential M, a convenient property in detailed studies on root water uptake (Raats, 1977; de Jong van Lier at al., 2008; Pinheiro et al., 2018). M (m^2 d^{-1}) is defined as the integral of the hydraulic conductivity function $K(h)$ (m d^{-1}) over a pressure head interval starting at an arbitrary reference pressure head h_{ref} (m):

$$M = \int_{h_{ref}}^{h} K(h)dh \quad (6)$$

Pinheiro et al. (2018) proposed to determine the limiting soil hydraulic condition as the onset of the falling rate phase of transpiration. For a layered soil, they obtained:

$$M_{lim} = \frac{pT_p}{\pi \sum_{i=1}^{k} L_i R_i} \quad (7)$$

where M_{lim} (m^2 d^{-1}) is the limiting matric flux potential, T_p is the potential transpiration rate (m d^{-1}), k is the number of soil layers, L_i (m) and R_i (m^{-2}) are the thickness and active root length density (RLD) for layer i. The value of an empirical constant p was calibrated to be equal to 5.3 when using $h_{ref} = -150$ m by Pinheiro et al. (2018). To calculate M_{lim} using Eq. (7), the following hypothetical scenario with an active RLD decreasing with depth is defined: $T_p = 4{\cdot}10^{-3}$ m d^{-1}, $L_1 = 0.25$ m, $R_1 = 100$ m^{-2}, $L_2 = 0.35$ m, and $R_2 = 10$ m^{-2}. Using these values, the resulting M_{lim} equals 2.37 10^{-4} m^2 d^{-1}. The T_p rate was chosen to represent an average subtropical condition under moderate temperature (Allen et al., 1998), while the active RLD values were based on the scenarios simulated by de Jong van Lier et al. (2006).

To determine the matric flux potential at wilting point, M_{wp}, T_p in Eq. (7) was substituted by a minimum (residual) transpiration at wilting point $T_{wp} = fT_p$, allowing a dynamic prediction of the wilting point. We used $f = 0.01$, resulting in $M_{wp} = 2.37\ 10^{-6}$ m^2 d^{-1}. The value for factor $f = 0.01$ is arbitrary, but was considered reasonable since a residual transpiration is maintained due to epidermal conductance (water loss through incompletely closed stomata and cuticular conductance) when the soil available water has been completely depleted (Sinclair and Ludlow, 1986; Sinclair et al., 2005). As discussed in Sinclair and Ludlow (1986), this residual transpiration can vary considerably among species.

M is uniquely correlated to θ and h. The M-θ-h relations are available for several standard soil hydraulic property models (including the van Genuchten functions) and M_{lim} or M_{wp} can be easily converted in corresponding values of water contents or pressure heads.

3. Results and discussion

3.1. Hypothetical experiment

Table 2 shows the overall performance of the parameter optimization with the objective function (Φ) defined in terms of $\theta(t)$ or $h(t)$ for selected initial parameter estimates.

Despite the inserted noise in $h(t)$ and $\theta(t)$ used to define the objective function Φ, the inverse solution repeatedly converged to a set of soil hydraulic parameters comparable to the original true set, producing low values of Φ and *RMSE* for all three initial parameter estimates. Although some optimized parameters, especially α, showed differences with original values, depending on the initial estimate, the general performance of the inverse solution was quite satisfactory. In general, both types of Φ produced similar fitted parameter values, indicating that the $\theta(t)$ dataset contains, similarly to the $h(t)$ dataset, substantial information for the determination of *SHP* using the inverse optimization approach (Ritter et al., 2003; Vereecken et al., 2008; Ines and Mohanty, 2008; Bourgeois et al., 2016). The lack of exactness for individual VGM parameters does not seem to be an essential issue (Bezerra-Coelho et al., 2018). For instance, Siltecho et al. (2015)

Table 2
Inverse optimization results for hypothetical evaporation experiments with Clay and Sandy Loam soils and with a normally distributed noise imposed on the virtual dataset of $h(t)$ and $\theta(t)$. Different sets of initial parameter estimates corresponding to different texture classes from ROSETTA (Schaap et al., 2001) were used.

Case	Initial estimate	θ_r —$m^3\ m^{-3}$—	θ_s	α m^{-1}	n –	K_s $m\ d^{-1}$	λ –	Φ –	*RMSE*
True parameters	**Clay**	**0.068**	**0.380**	**0.800**	**1.090**	**0.048**	**0.500**	–	–
$h(t)$	Clay	–	0.380	0.800	1.090	0.048	0.498	$1.4{\cdot}10^{-6}$	$2.6{\cdot}10^{-5}$ m
$\theta(t)$		–	0.380	0.804	1.090	0.048	0.504	$8.7{\cdot}10^{-6}$	$5.9{\cdot}10^{-5}\ m^3\ m^{-3}$
$h(t)$	Silt	–	0.379	0.760	1.091	0.044	0.472	$7.3{\cdot}10^{-6}$	$5.9{\cdot}10^{-5}$ m
$\theta(t)$		–	0.380	0.737	1.091	0.046	0.665	$9.0{\cdot}10^{-6}$	$6.0{\cdot}10^{-5}\ m^3\ m^{-3}$
$h(t)$	Sandy Clay	–	0.360	0.552	1.108	0.024	0.001	$1.0{\cdot}10^{-3}$	$7.7{\cdot}10^{-4}$ m
$\theta(t)$		–	0.380	0.549	1.096	0.039	1.181	$9.6{\cdot}10^{-6}$	$6.2{\cdot}10^{-5}\ m^3\ m^{-3}$
True parameters	**Sandy Loam**	**0.065**	**0.410**	**7.500**	**1.890**	**1.061**	**0.500**	–	–
$h(t)$	Sandy Loam	–	0.410	7.500	1.891	1.064	0.500	$8.0{\cdot}10^{-4}$	$3.6{\cdot}10^{-4}$ m
$\theta(t)$		–	0.409	7.436	1.910	1.073	0.523	$6.6{\cdot}10^{-3}$	$1.0{\cdot}10^{-3}\ m^3\ m^{-3}$
$h(t)$	Loamy sand	–	0.409	7.534	1.893	1.081	0.497	$8.1{\cdot}10^{-4}$	$3.6{\cdot}10^{-4}$ m
$\theta(t)$		–	0.409	7.134	2.041	1.186	0.737	$7.6{\cdot}10^{-3}$	$1.1{\cdot}10^{-3}\ m^3\ m^{-3}$
$h(t)$	Silt	–	0.409	7.487	1.900	1.054	0.490	$8.1{\cdot}10^{-4}$	$3.6{\cdot}10^{-4}$ m
$\theta(t)$		–	0.410	7.634	1.834	1.039	0.398	$6.8{\cdot}10^{-3}$	$1.0{\cdot}10^{-3}\ m^3\ m^{-3}$

demonstrated that individual values of the VGM parameters, especially the parameters n and K_s, are highly dependent on the measurement technique. However, this individual dependency is not translated into noticeable differences in further simulations of state variables.

The highest parameter correlation was between α and n when minimizing $\Phi[\theta(t)]$, and between α and K_s when minimizing $\Phi[h(t)]$ (Table 3).

Although the level of uncertainty is expected to be higher for parameters that display a high correlation (Šimůnek et al., 1998), even these optimized parameters were close to their true values (see Table 2). The tortuosity factor (λ), which exhibited a relatively low correlation with the other parameters, produced the highest deviations from its true values, both for $\Phi[\theta(t)]$ and $\Phi[h(t)]$. Initial estimates close to the true values always produced a good fit. Similar findings using the same type of Φ were reported by Šimůnek et al. (1998) and Siltecho et al. (2015), who found that unrealistic fits can be avoided by choosing initial parameter values reasonably close to their true values.

3.2. Soil hydraulic properties of real soils

Optimized soil hydraulic parameters for all analyzed soils are given in Table 4. A satisfactory agreement (relatively low standard errors) was observed between the replicates. This is worth noting because undisturbed soil samples taken from field sites may naturally exhibit a high heterogeneity.

The VGM description of soil hydraulic properties only accounts for the capillary water retention and conductivity (Peters, 2013) and may produce an erroneous description in the very dry range. Although the experiments were carried out for about three weeks, down to very dry conditions when daily sample weight changes reached negligible values, we did not incorporate all final measurements into Φ of Hydrus-1D. After performing several tests, we concluded that for the soil samples and laboratory conditions, 10–12 days of water content measurements were enough to reach pressure heads in the range of −140 to −180 m during the optimization process.

Table 3
Correlation matrix for the inverse solution for the hypothetical experiment (Clay soil) with Φ defined in terms of $\theta(t)$ and $h(t)$.

Definition of Φ	Parameter	θ_s	α	n	K_s	λ
$\theta(t)$	θ_s	1.0	–	–	–	–
	α	0.22	1.0	–	–	–
	n	−0.20	−0.99	1.0	–	–
	K_s	0.05	0.48	−0.44	1.0	–
	λ	−0.22	−0.60	0.64	0.40	1.0
$h(t)$	θ_s	1.0	–	–	–	–
	α	−0.66	1.0	–	–	–
	n	−0.41	−0.39	1.0	–	–
	K_s	−0.51	0.94	−0.47	1.0	–
	λ	0.53	−0.01	−0.57	0.30	1.0

The only VGM parameter not fitted during the inverse simulations was θ_r. In general, θ_r and θ_s are assumed to be easily determined by direct measurements. Once determined, they can be either introduced in the objective function in a Bayesian sense or used directly as true values, reducing the overall parameter uncertainty (Siltecho et al., 2015). Šimůnek et al. (1998) found a high correlation between parameters θ_r and n and observed a substantial improvement in the inverse solution when θ_r was either inserted in the objective function or fixed at its true value. In our case, as we kept the experiment running until quasi air-dry conditions, the last recorded value of water content was set as the true value of θ_r.

Regarding θ_s, it may be unrealistic to consider the measured total porosity to be a proxy for θ_s for field conditions, because it is very unlikely for a soil profile, or even a soil sample, to reach the state of full saturation due to water repellency and entrapped or dissolved air (Pachepsky et al., 2001; Vereecken et al., 2010). In our experiments, a low correlation between θ_s and other parameters was observed for all soils (ranging from −0.001 to 0.3) and θ_s was thus kept as a fitting parameter. Fitted θ_s values were similar to the measured initial total water content in the soil samples.

The λ parameter, which is related to the tortuosity and pore space connectivity, is usually assumed to be equal to 0.5 according to Mualem (1976), but its true value is hardly ever determined over the full range of pressure heads. Since for inverse parameter optimization problems, reducing the number of fitting parameters increases the uniqueness and stability of the solution, a fixed λ of 0.5 has often been adopted in studies dealing with parameter optimization (e.g., Šimůnek et al., 1998; Siltecho et al., 2015; Brunetti et al., 2016). Although the physical meaning of λ is frequently questioned (e.g., Vereecken et al., 2010; Peters, 2013), the unsaturated hydraulic conductivity function (K) is highly sensitive to λ values (Van Dam et al., 1994; Schaap and Leij, 2000), especially in the near-wilting range, and the standard practice of using fixed λ may lead to underpredictions of K and poor simulations of crop water availability (de Jong van Lier et al., 2015). For all soil samples used in this research, fitted λ values were either zero or close to zero (Table 4). Similar results were reported in de Jong van Lier (2017) and Pinheiro et al. (2018) for tropical soils. As discussed in Vereecken et al. (2010), many studies have revisited the parameter λ and found values strongly deviating from 0.5.

The average K_s for the coarse (sand content > 80%) and fine textured soils was 0.40 ± 0.39 (± standard deviation) m d^{-1} and

Table 4
Optimized van Genuchten-Mualem parameters and statistics of Hydrus-1D inverse solutions: average values of the objective function (Φ) and root mean squared error (*RMSE*). The values between parentheses are the standard errors representative of the five replicas.

Site	Layer	θ_r[1]	θ_s	α	n	K_s	λ	Φ	*RMSE*
		$m^3 m^{-3}$		m^{-1}	–	$m\ d^{-1}$	–	–	$m^3 m^{-3}$
1	0.00-0.15	0.025 (0.0021)	0.324 (0.0024)	2.221 (0.0930)	1.622 (0.0201)	0.473 (0.0654)	0.100 (0.0639)	0.031	0.023
	0.30-0.45	0.025 (0.0019)	0.320 (0.0024)	2.816 (0.1230)	1.565 (0.0168)	0.520 (0.0721)	0.006 (0.0567)	0.039	0.029
2	0.00-0.15	0.042 (0.0010)	0.344 (0.0016)	2.031 (0.0420)	1.788 (0.0091)	0.211 (0.0115)	0.000 (−)	0.017	0.016
	0.30-0.45	0.034 (0.0010)	0.344 (0.0017)	2.693 (0.0480)	2.160 (0.2045)	0.570 (0.0501)	0.028 (0.0358)	0.025	0.019
3	0.00-0.15	0.046 (0.0140)	0.395 (0.0011)	0.950 (0.0340)	1.206 (0.0133)	0.070 (0.0100)	−0.011 (0.1261)	0.022	0.020
	0.30-0.45	0.069 (0.0072)	0.415 (0.0013)	1.783 (0.0840)	1.180 (0.0066)	0.285 (0.0350)	0.00 (−)	0.023	0.022
4	0.00-0.15	0.049 (0.0104)	0.378 (0.0010)	1.379 (0.0480)	1.202 (0.0107)	0.136 (0.0170)	−0.015 (0.1005)	0.027	0.022
	0.30-0.45	0.060 (0.0046)	0.372 (0.0010)	1.747 (0.0560)	1.173 (0.0044)	0.150 (0.0130)	0.000 (−)	0.026	0.025
5	0.00-0.15	0.042 (0.0060)	0.350 (0.0013)	1.080 (0.0050)	1.242 (0.0094)	0.094 (0.0110)	0.000 (−)	0.025	0.020
	0.30-0.45	0.046 (0.0053)	0.344 (0.0010)	1.400 (0.0290)	1.217 (0.0066)	0.301 (0.0220)	−0.002 (0.0585)	0.015	0.022
6	0.00-0.15	0.030 (0.0068)	0.362 (0.0010)	0.888 (0.0330)	1.208 (0.0076)	0.096 (0.0100)	0.000 (−)	0.015	0.021
	0.30-0.45	0.028 (0.0095)	0.350 (0.0010)	1.608 (0.0610)	1.197 (0.0100)	0.102 (0.0130)	−0.010 (0.0934)	0.022	0.023
7	0.00-0.15	0.048 (0.0066)	0.410 (0.0011)	1.482 (0.0600)	1.183 (0.0060)	0.233 (0.0240)	0.000 (−)	0.024	0.025
	0.30-0.45	0.054 (0.0107)	0.415 (0.0020)	1.129 (0.0670)	1.201 (0.0107)	0.293 (0.0460)	0.000 (−)	0.025	0.028
8	0.00-0.15	0.053 (0.0154)	0.427 (0.0012)	1.205 (0.0440)	1.192 (0.0126)	0.217 (0.0320)	0.261 (0.1443)	0.041	0.028
	0.30-0.45	0.063 (0.0147)	0.419 (0.0010)	0.783 (0.0210)	1.180 (0.0109)	0.054 (0.0060)	−0.012 (0.1236)	0.073	0.036
9	0.00-0.15	0.034 (0.0022)	0.290 (0.0015)	2.211 (0.0850)	1.471 (0.0141)	0.515 (0.0590)	0.005 (0.0548)	0.025	0.021
	0.30-0.45	0.031 (0.0041)	0.306 (0.0023)	2.361 (0.1410)	1.397 (0.0180)	0.316 (0.0550)	0.013 (0.0828)	0.039	0.027
10	0.00-0.15	0.040 (0.0029)	0.357 (0.0054)	4.272 (0.3800)	1.428 (0.0148)	0.502 (0.1040)	0.000 (−)	0.080	0.037
	0.30-0.45	0.039 (0.0028)	0.368 (0.0040)	2.752 (0.1830)	1.455 (0.0135)	1.586 (0.2420)	0.000 (−)	0.090	0.039
11	0.00-0.15	0.036 (0.0011)	0.351 (0.0026)	3.096 (0.0980)	1.817 (0.0188)	0.034 (0.0040)	0.040 (0.0491)	0.048	0.029
	0.30-0.45	0.035 (0.0013)	0.368 (0.0046)	4.738 (0.2340)	1.727 (0.0197)	0.680 (0.1260)	0.194 (0.0603)	0.060	0.030

[1] θ_r was fixed at its true value during the inverse solutions.

$0.15 \pm 0.09\ m\ d^{-1}$, respectively. K_s showed a positive correlation with α (0.3 to 0.8) and negative correlation with n (-0.2 to -0.9) for most replicates and for all soil textures. However, the correlation with λ was low and ranged from negative to positive values. In a broad sense, the parameters n and α are empirical and determine the shape of the retention curve. Van Genuchten (1980) related α to the average pore sizes, and a larger α enhances K_s. Šimůnek et al. (1998) also found a strong negative correlation between fitted K_s and the parameter n for a specific scenario. The drop of the hydraulic conductivity near saturation is controlled by the n parameter to a much higher extent than by the λ parameter (Vereecken et al., 2010).

In general, several studies have shown that many uncertainties are involved in the K_s fitting of Eq. (3), and similar to λ, n, and α, K_s must be treated and interpreted as an empirical shape parameter (Schaap and Leij, 2000; Vereecken et al., 2010). In fact, according to Schaap and Leij (2000), fitted K_s values are usually almost one order of magnitude lower than independent measurements of the saturated hydraulic conductivity. Eq. (3) does not account for macropore flow, which is expected to take place under pressure head values higher than −10 cm (Jarvis, 2007; Weynants et al., 2009), and therefore, using independent measurements of the saturated hydraulic conductivity in Eq. (3) is problematic.

A very good agreement was found between mean soil water contents of the soil cores obtained from measured core weight changes over time and corresponding simulated values. The average values of *NSE* and *RMSE* were 0.956 ± 0.037 and 0.018 ± 0.007 $m^3 m^{-3}$, respectively, for the coarse-textured soils, and 0.903 ± 0.043 and 0.024 ± 0.005 $m^3 m^{-3}$, respectively, for the fine-textured soils. Since measured values of mean water contents obtained during the experiments from weight records were not used in the objective function of the inverse solution, this good agreement indicates that the optimized sets of soil hydraulic parameters can predict transient water flow process in the evaluated soils with relatively robustness.

Using Eqs. (2) and (3) together with the optimized VGM parameters from Table 4, water contents and hydraulic conductivities for selected values of the pressure head in the range of crop available water were calculated for the surface layer of the evaluated soils (Table 5). In general, the known effect of texture on the soil hydraulic behavior can be readily identified. For coarser textured soils (loamy fine sands), a sharp drop in θ and K can be observed for pressure heads close to saturation. For these soils, K at $h = -150$ m reaches values three to four orders of magnitude lower than for finer textured soils. In terms of root water uptake in water-limited scenarios, a non-stressed condition is attained when a local drop in the K value is compensated by an increase in the hydraulic gradient between the bulk soil and the root surface. A sharp gradient increase will force the root system to exert a very negative pressure head even when the bulk soil is still relatively wet, making the onset of the drought stress (h_{lim}) to occur at a less negative pressure head (de Jong van Lier et al., 2006; Pinheiro et al., 2018). Consequently, according to results presented in Table 5, the most restrictive surface soil layer for root water uptake is site 11, having the lowest values of K over an entire dry range of pressure heads. The importance of K for unsaturated conditions on the root water uptake process justifies the need of its determination with a good accuracy in the dry range. De Jong van Lier et al. (2015) showed in detail that without reliable soil hydraulic properties, especially K, drought stress cannot be correctly predicted in most cases.

3.3. Comparison of retention curves obtained using the pressure plate apparatus and the inverse solutions

Retention curves (*RC*) obtained using the inverse parameter estimation corresponded relatively well to those obtained using the pressure plate apparatus (*PPA*). Fig. 3 shows four examples of *RC* obtained using the *PPA* and the inverse solution together with independent pairs of $h(\theta)$ measured using a dew point device.

For the coarse-textured soils (sites 1–2 and 9–11), the two approaches produced very similar curves in the entire range of soil water contents. On the other hand, for fine-textured soils (sites 3–8), *RC* obtained using the *PPA* overestimated soil water contents in the dry range. Dew point measurements performed on independent samples subjected to a pressure head of −150 m on the *PPA* for 15, 30, and 100 days matched values obtained by the inverse solution, suggesting the *PPA* values are overestimated at lower pressure heads for fine textured soils (Fig. 3). The three dew point measurements after different equilibrium times were practically the same. Several studies discuss errors in low pressure head values of the *RC* determined using the *PPA*, especially for fine-textured soils (e.g., Cresswell et al., 2008; Bitelli and Flury, 2009;

Table 5
Water contents and hydraulic conductivities for some values of pressure heads for the surface soil layer of the 11 analyzed soils (values calculated from soil hydraulic parameters in Table 4).

Site	Texture class	Pressure head (m)									
		−0.1	−1.0	−3.3	−10	−150	−0.1	−1.0	−3.3	−10	−150
		θ ($m^3 m^{-3}$)					K ($m\ d^{-1}$)				
1	Loamy fine sand	0.315	0.191	0.110	0.068	0.033	$1.8{\cdot}10^{-1}$	$3.5{\cdot}10^{-3}$	$9.0{\cdot}10^{-5}$	$2.4{\cdot}10^{-6}$	$3.2{\cdot}10^{-10}$
2	Sandy Loam	0.337	0.197	0.108	0.070	0.045	$1.1{\cdot}10^{-1}$	$2.3{\cdot}10^{-3}$	$4.3{\cdot}10^{-5}$	$8.6{\cdot}10^{-7}$	$5.4{\cdot}10^{-11}$
3	Clay	0.392	0.358	0.311	0.263	0.172	$1.1{\cdot}10^{-2}$	$9.5{\cdot}10^{-4}$	$9.9{\cdot}10^{-5}$	$8.3{\cdot}10^{-6}$	$1.3{\cdot}10^{-8}$
4	Clay	0.373	0.332	0.285	0.241	0.161	$1.6{\cdot}10^{-2}$	$9.5{\cdot}10^{-4}$	$8.4{\cdot}10^{-5}$	$6.7{\cdot}10^{-6}$	$1.1{\cdot}10^{-8}$
5	Sandy Clay	0.346	0.309	0.260	0.213	0.132	$1.7{\cdot}10^{-2}$	$1.3{\cdot}10^{-3}$	$1.2{\cdot}10^{-4}$	$9.1{\cdot}10^{-6}$	$1.2{\cdot}10^{-8}$
6	Clay loam	0.359	0.328	0.285	0.238	0.150	$1.5{\cdot}10^{-2}$	$1.5{\cdot}10^{-3}$	$1.6{\cdot}10^{-4}$	$1.3{\cdot}10^{-5}$	$2.1{\cdot}10^{-8}$
7	Clay	0.404	0.360	0.313	0.268	0.183	$2.2{\cdot}10^{-2}$	$1.2{\cdot}10^{-3}$	$1.1{\cdot}10^{-4}$	$9.0{\cdot}10^{-6}$	$1.6{\cdot}10^{-8}$
8	Clay	0.422	0.381	0.332	0.283	0.191	$2.5{\cdot}10^{-2}$	$1.7{\cdot}10^{-3}$	$1.6{\cdot}10^{-4}$	$1.2{\cdot}10^{-5}$	$1.8{\cdot}10^{-8}$
9	Loamy fine sand	0.282	0.196	0.133	0.093	0.051	$1.4{\cdot}10^{-1}$	$3.5{\cdot}10^{-3}$	$1.4{\cdot}10^{-4}$	$5.7{\cdot}10^{-6}$	$2.0{\cdot}10^{-9}$
10	Loamy fine sand	0.333	0.204	0.141	0.103	0.060	$6.4{\cdot}10^{-2}$	$6.1{\cdot}10^{-4}$	$2.3{\cdot}10^{-5}$	$9.9{\cdot}10^{-7}$	$4.3{\cdot}10^{-10}$
11	Loamy fine sand	0.335	0.155	0.083	0.055	0.038	$1.4{\cdot}10^{-2}$	$9.1{\cdot}10^{-5}$	$1.3{\cdot}10^{-6}$	$2.3{\cdot}10^{-8}$	$1.1{\cdot}10^{-12}$

Solone et al., 2012; Roy et al., 2018). The main causes of *PPA* errors reported in these studies are related to a poor soil-plate contact caused by drying, as well as to a low unsaturated hydraulic conductivity.

The difference between curves at near saturation was more evident for fine-textured soils. The saturation of some of the soil cores used in the *PPA* was up to 10–15% higher than of those (300 cm^3) used in evaporation experiments. Samples in evaporation experiments were about 5 times larger in volume than *PPA* samples, and larger samples are more representative of field conditions, i.e., more prone to water repellency and dissolved or entrapped air. According to Vereecken et al. (2010), an accurate description of *RC* in the wet range remains a challenge due to regular failures in determining the soil water content close to saturation. Saturated water contents are usually measured in the laboratory on small soil samples used in the *PPA* or set equal to the total porosity, which is calculated from soil particle and soil bulk densities. Such values of θ_s when extrapolated to transient field conditions may lead to unreliable simulations, as reported in Vereecken et al. (2010), where discontinuities in the non-wetting phase near saturation (when air cannot access all the medium) cause worse correlations of the unsaturated hydraulic conductivity with water retention at water contents higher than 85% of the saturated value.

3.4. Crop water availability evaluated for soils and land use

Soil hydraulic properties determine all processes related to soil water flow, including drainage and flow towards roots, which is involved in crop water uptake. Nevertheless, threshold values for crop available water (commonly expressed as field capacity, a transpiration limiting condition, and a wilting point) are usually predicted using empirically fixed values of pressure head. In a more process-based and dynamic approach, Table 6 shows a direct application of soil hydraulic parameters (Table 4) to calculate pressure head thresholds that define crop water availability for a specific scenario of root length density and crop transpiration.

The pressure head at field capacity (using the 1 mm d^{-1} bottom flux criterion) showed a considerable variability among soils and layers,

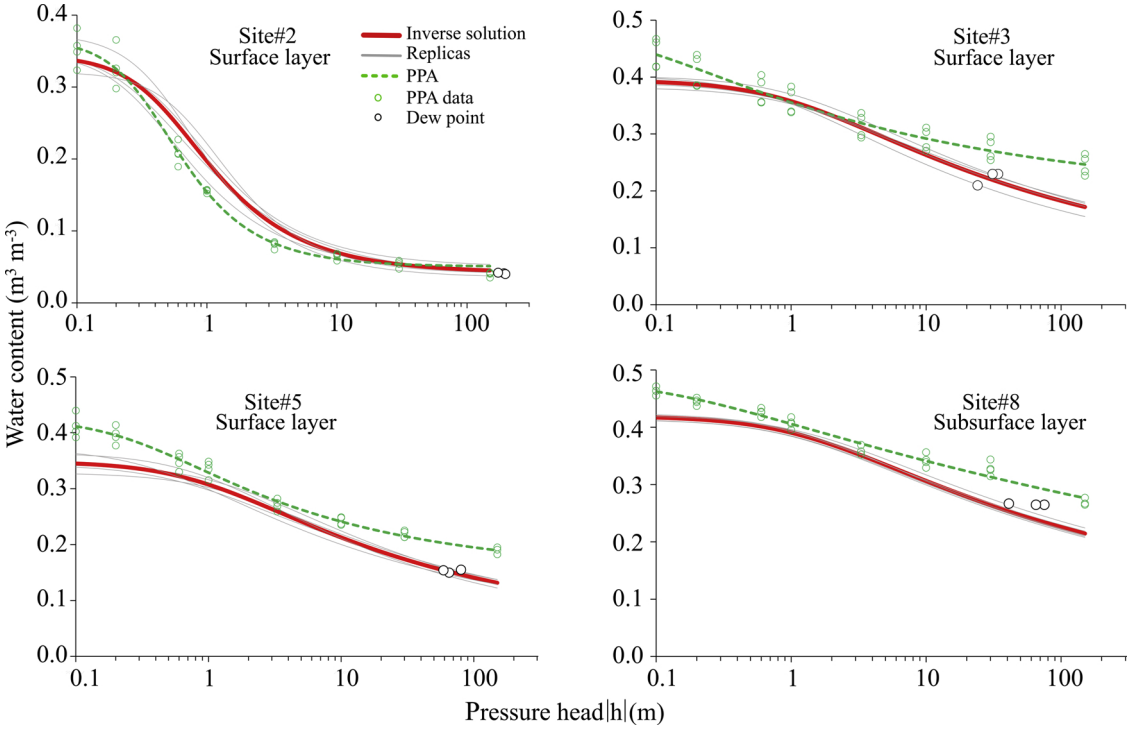

Fig. 3. Water retention curves obtained using the inverse parameter estimation and the pressure plate apparatus (PPA) together with dew point measurement data.

Table 6
Pressure heads (h) and water contents (θ) corresponding to dynamic criteria for field capacity (q_{60} = 1 mm d^{-1}), limiting conditions (M_{lim} = 2.37·10^{-4} m^2 d^{-1}), and wilting conditions (M_{wp} = 2.37·10^{-6} m^2 d^{-1}).

Site	Layer	h_{fc}	h_{lim}	h_{wp}	θ_{fc}	θ_{lim}	θ_{wp}
		m			m^3 m^{-3}		
1	0.00-0.25	−1.4	−2.6	−19	0.166	0.124	0.054
	0.25-0.60	−1.2	−2.1	−19	0.166	0.130	0.056
2	0.00-0.25	−1.3	−1.9	−11	0.173	0.144	0.067
	0.25-0.60	−1.1	−1.3	−5	0.116	0.102	0.048
3	0.00-0.25	−1.1	−3.6	−74	0.355	0.308	0.191
	0.25-0.60	−0.9	−3.2	−72	0.366	0.317	0.214
4	0.00-0.25	−0.8	−3.1	−67	0.339	0.288	0.181
	0.25-0.60	−0.6	−1.9	−53	0.339	0.305	0.203
5	0.00-0.25	−1.5	−3.9	−71	0.293	0.253	0.150
	0.25-0.60	−1.3	−5.6	−90	0.289	0.234	0.150
6	0.00-0.25	−0.8	−5.2	−90	0.334	0.266	0.163
	0.25-0.60	−0.6	−1.8	−47	0.316	0.279	0.165
7	0.00-0.25	−1.7	−3.8	−79	0.358	0.307	0.199
	0.25-0.60	−1.5	−7.7	−107	0.356	0.285	0.192
8	0.00-0.25	−0.9	−4.9	−85	0.385	0.314	0.207
	0.25-0.60	−0.7	−3.7	−81	0.397	0.346	0.231
9	0.00-0.25	−1.3	−3.4	−36	0.180	0.132	0.067
	0.25-0.60	−1.1	−2.5	−32	0.207	0.164	0.080
10	0.00-0.25	−1.9	−1.3	−15	0.168	0.191	0.093
	0.25-0.60	−1.8	−4.5	−48	0.194	0.143	0.075
11	0.00-0.25	−0.8	−0.4	−3	0.174	0.235	0.088
	0.25-0.60	−0.7	−0.9	−5	0.163	0.151	0.067

ranging from −1.9 m to −0.6 m. However, in general, the −1 m threshold used in the "static" approach seems to be a reasonable proxy. Transpiration limiting pressure heads vary from −1 to −8 m, which is comparable to the order of magnitude used for the value of h_3 in the Feddes et al. (1978) reduction function (see the compilation by Taylor and Ashcroft, 1972) and in the same order of magnitude as the criterion of 70–80% of θ_{fc} (Zuo et al., 2006; Shi et al., 2015). Pressure head values at wilting point ranged from −3 to −107 m, with a considerable variability among soils and layers. As highlighted by Bouma (2018), the common value of −150 m for a wilting point (determined in the 1930s) does not apply for many combinations of crops and soils, where wilting may occur closer to saturation.

The general effect of the "dynamic" approach can be seen when comparing the corresponding values of total and readily available water

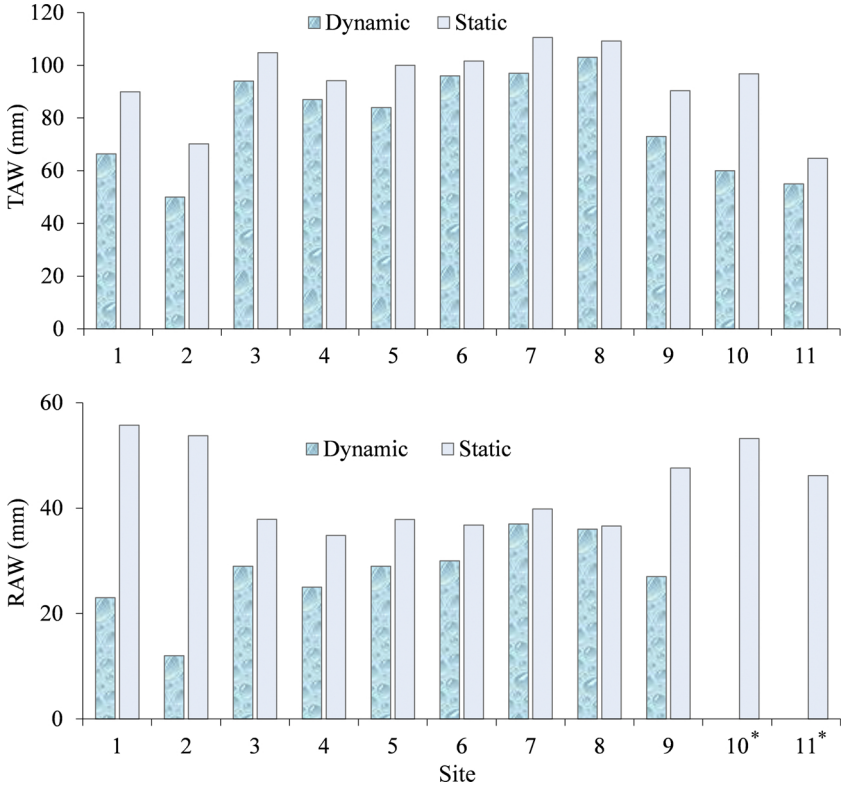

Fig. 4. Total and readily available water (TAW and RAW) determined using "dynamic" and "static" criteria for pressure head thresholds in the 11 evaluated soils. The asterisk indicates non-existent RAW in the surface layer.

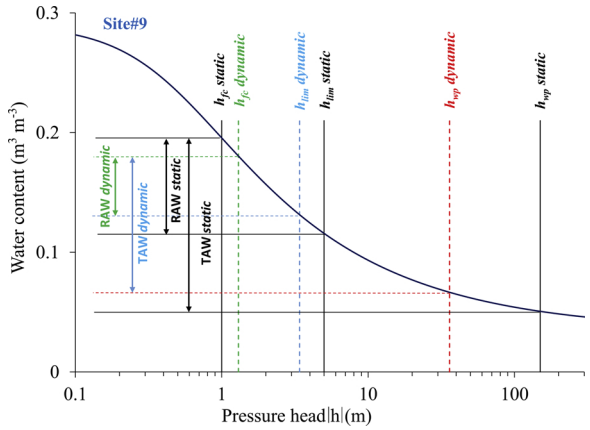

Fig. 5. Retention curve for the surface layer of site 9, illustrating differences between typical water contents and available water (TAW and RAW) obtained using the "static" and "dynamic" pressure head approaches.

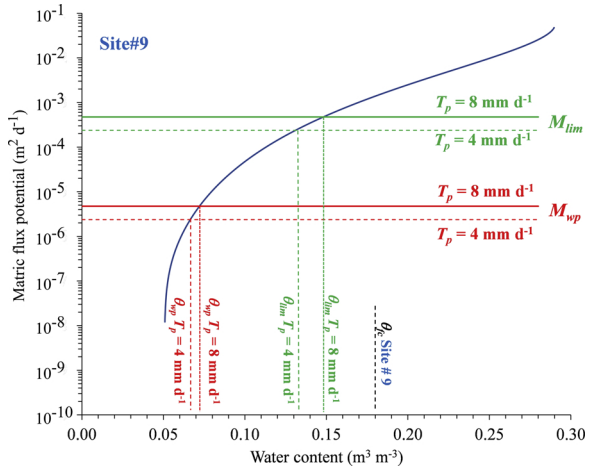

Fig. 6. Effect of potential transpiration on the limiting matric flux potential and the lower thresholds of RAW and TAW (θ_{lim} and θ_{wp}) for the soil at Site 9.

(TAW and RAW) (Fig. 4). For fine-textured soils (sites 3–8), the TAW and RAW values calculated using the "static" pressure heads are higher, although very similar, than the values simulated using the "dynamic" approach for the chosen scenario. On the other hand, the TAW and RAW values for coarse-textured soils estimated using the "dynamic" approach are considerably lower than for the "static" method. In the surface layer of sites 10 and 11 (both coarse-textured soils), θ_{fc} was lower than θ_{lim}, causing a non-existing RAW. This fact (i.e., when drainage quickly produces a water content limiting transpiration) is physically plausible and may be expected in soils with a higher α and n, i.e., coarse-textured soils (soils with a high macroporosity and narrow pore-size distribution), in which drainage of water leads to a sharp drop in the pressure head. In these soils under rainfed condition, transpiration and crop growth would be always limited, except for a (short) time period immediately following rainfall. In fact, de Jong van Lier (2017) showed that a considerable fraction of crop water uptake occurs at water contents higher than field capacity, and thus a non-existing RAW does not necessary mean that the crops will always be under stress.

Fig. 5 shows details about the differences depicted in Fig. 4 for site 9. Whereas pressure head thresholds determined using the "dynamic" approach take into consideration soil hydraulic properties (e.g., retention and unsaturated hydraulic conductivity), rooting characteristics, and the atmospheric demand, the "static" values are based solely on empirically determined "traditional" values, making them unable to distinguish between commonly varying features in soil, crops, and atmosphere.

The "dynamic" approach not only considers the role of unsaturated hydraulic properties, but it also allows for the direct analysis of how the transpiration rate and root length density affect the onset of drought stress. In the same soil (i.e., the same hydraulic properties), crops with a higher RLD maintain the water potential at the root surface closer to the average pressure head in the surrounding soil since the flux density toward the root surface to meet the transpiration rate is smaller, and h_{lim} is lower, corresponding to a drier soil (de Jong van Lier et al., 2006; dos Santos et al., 2017; Pinheiro et al., 2018). The effect of T_p on the lower limits of TAW and RAW determined using the "dynamic" method is shown in Fig. 6. Higher T_p values lower the soil available water since the drought stress and the wilting point will occur closer to the upper limit of field capacity.

The effect of land use on crop water availability was more noticeable for coarse-textured soils (sites 1–2 and 9–11). For fine-textured soils, the RAW values were practically identical for the same soils with different land use. For three forest sites (4, 7, and 10), contrary to what would commonly be expected, the RAW values were very similar to the values of the neighboring soil under intensive agricultural land use. In general, forests are assumed to have higher organic matter content (Gajić, 2013), which may affect soil hydraulic properties and enhance the soil water-holding capacity. Siltecho et al. (2015) found a negligible influence of different land uses (forest, rubber plantation, and grass) on soil hydraulic properties. Minasny and McBratney (2018) carried out a meta-analysis investigation and concluded that the effect of organic matter on total available water was very modest. These authors used "static" pressure heads to retrieve TAW, which may have biased their final conclusions. As commented by Bouma (2018), soil-water flow in the vadose zone is a very dynamic process determined mainly by hydraulic properties, root depth, transpiration, and the rainfall pattern. Therefore, Richards-equation based models require more data, but are more powerful in combining soil, plant, and climate dynamically than models that apply a simpler approach with fixed threshold values (field capacity, limiting condition, and wilting point) for crop available water.

4. Conclusions

Using experimental and numerical protocols for determining soil hydraulic properties and assessing a process-based estimation of crop water availability, we conclude that:

1 An evaporation experiment performed with a non-invasive technique (gamma-ray attenuation) to measure water contents from near-saturation (~ −0.1 m pressure head) to the dry range (~ −150 m) allowed the determination of unsaturated soil hydraulic properties over the entire range by inverse modeling.
2 The determined soil hydraulic parameters could be employed to calculate crop available water using the traditional "static" pressure head method, as well as a multilayer "dynamic" approach. Considering a specific scenario of atmospheric demand and active root length density, the "static" and "dynamic" approaches performed similarly for the fine-textured soils. However, for the coarse-textured soils, the two approaches diverged significantly. Overall, the "dynamic" method allows incorporating important system characteristics (atmospheric demand and crop properties) and soil hydraulic properties in a transparent (process-based) way, contrarily to the "static" method.
3 No tendency could be revealed for crop water availability under different land uses, and, in general, crop available water for soils under forest use was very similar to their counterparts under agricultural use.

Acknowledgment

This work was supported by the São Paulo Research Foundation (FAPESP) (grant numbers 2016/16128-4 and 2017/17793-4).

References

Abbaspour, K.C., Schulin, R., van Genuchten, M.Th., 2001. Estimating unsaturated soil hydraulic parameters using ant colony optimization. Adv. Water Resour. 24, 827–841. https://doi.org/10.1016/S0309-1708(01)00018-5.

Allen, R.G., Pereira, L.S., Raes, D., Smith, M., 1998. Crop Evapotranspiration - Guidelines for Computing Crop Water Requirements. FAO Irrig. Drain. Pap. 56. FAO, Rome.

Bezerra-Coelho, C.R., Zhuang, L., Barbosa, M.C., Soto, M.A., van Genuchten Th, M., 2018. Further tests of the HYPROP evaporation method for estimating the unsaturated soil hydraulic properties. J. Hydrol. Hydromech. 66, 161–169. https://doi.org/10.1515/johh-2017-0046.

Bittelli, M., Flury, M., 2009. Errors in water retention curves determined with pressure plates. Soil Sci. Soc. Am. J. 73, 1453–1460. https://doi.org/10.2136/sssaj2008.0082.

Bouma, J., 2018. Comment on: B. Minasny & A.B. Mc Bratney. 2018. Limited effect of organic matter on soil available water capacity. Eur. J. Soil Sci. 69, 154. https://doi.org/10.1111/ejss.12509.

Bourgeois, O.Le., Bouvier, C., Brunet, P., Ayral, P.A., 2016. Inverse modeling of soil water content to estimate the hydraulic properties of a shallow soil and the associated weathered bedrock. J. Hydrol. 541, 116–126. https://doi.org/10.1016/j.jhydrol.2016.01.067.

Brooks, R.H., Corey, A.T., 1964. Hydraulic Properties of Porous Media: Hydrology Papers. Colorado State University, Fort Collins, Colorado.

Brunetti, G., Šimůnek, J., Piro, P., 2016. A comprehensive numerical analysis of the hydraulic behavior of a permeable pavement. J. Hydrol. 540, 1146–1161. https://doi.org/10.1016/j.jhydrol.2016.07.030.

Cai, G., Vanderborgh, J., Couvreur, V., Mboh, C.M., Vereecken, H., 2018. Parameterization of root water uptake models considering dynamic root distributions and water uptake compensation. Vadose Zone J. 17, 160125. https://doi.org/10.2136/vzj2016.12.0125.

Campbell, G.S., 1974. A simple method for determining unsaturated conductivity from moisture retention data. Soil Sci. 117, 311–314.

Cresswell, H.P., Green, T.W., Mckenzie, N.J., 2008. The adequacy of pressure plate apparatus for determining soil water retention. Soil Sci. Soc. Am. J. 72, 41–49. https://doi.org/10.2136/sssaj2006.0182.

de Jong van Lier, Q., 2017. Field capacity, a valid upper limit of crop available water? Agric. Water Manage. 193, 214–220. https://doi.org/10.1016/j.agwat.2017.08.017.

de Jong van Lier, Q., Wendroth, O., 2016. Reexamination of the field capacity concept in a Brazilian Oxisol. Soil Sci. Soc. Am. J. 79, 9–19. https://doi.org/10.2136/sssaj2015.01.0035.

de Jong van Lier, Q., Metselaar, K., Van Dam, J.C., 2006. Root water extraction and limiting soil hydraulic conditions estimated by numerical simulation. Vadose Zone J. 5, 1264–1277. https://doi.org/10.2136/vzj2006.0056.

De Jong van Lier, Q., Wendroth, O., Van Dam, J.C., 2015. Prediction of winter wheat yield with the SWAP model using pedotransfer functions: an evaluation of sensitivity, parameterization and prediction accuracy. Agric. Water Manage. 154, 29–42. https://doi.org/10.1016/j.agwat.2015.02.011.

de Jong Van Lier, Q., Van Dam, J.C., Metselaar, K., De Jong, R., Duijnisveld, W.H.M., 2008. Macroscopic root water uptake distribution using matric flux potential approach. Vadose Zone J. 7, 1065–1078. https://doi.org/10.2136/vzj2007.0083.

De Willigen, P., Van Noordwijk, M., 1987. Roots, Plant Production and Nutrient Use Efficiency. Ph.D. diss. Wageningen University, the Netherlands.

Dos Santos, M.A., De Jong van Lier, Q., Van Dam, J.C., Bezerra, A.H.F., 2017. Benchmarking test of empirical root water uptake models. Hydrol. Earth Syst. Sci. 21, 473–493. https://doi.org/10.5194/hess-21-473-2017.

Durner, W., 1994. Hydraulic conductivity estimation for soils with heterogeneous pore structure. Water Resour. Res. 30, 211–223. https://doi.org/10.1029/93WR02676.

Durner, W., Iden, S.C., 2011. Extended multistep outflow method for the accurate determination of soil hydraulic properties near water saturation. Water Resour. Res. 47, W08526. https://doi.org/10.1029/2011WR010632.

Feddes, R.A., Kowalik, P.J., Zaradny, H., 1978. Simulation of Field Water Use and Crop Yield. Pudoc. Centre Agric. Publ. Doc., Wageningen.

Gajić, B., 2013. Physical properties and organic matter of Fluvisols under forest, grassland, and 100 years of conventional tillage. Geoderma 200–201, 114–119. https://doi.org/10.1016/j.geoderma.2013.01.018.

Gardner, W.R., Miklich, F.J., 1962. Unsaturated conductivity and diffusivity measurements by a constant flux method. Soil Sci. 93, 271–274.

Groenevelt, P.H., Grant, C.D., 2004. A new model for the soil-water retention curve that solves the problem of residual water contents. Eur. J. Soil Sci. 55, 479–485. https://doi.org/10.1111/j.1365-2389.2004.00617.x.

Ines, A.V.M., Mohanty, B.P., 2008. Near-Surface soil moisture assimilation for quantifying effective soil hydraulic properties under different hydroclimatic conditions. Vadose Zone J. 7, 39–52. https://doi.org/10.2136/vzj2007.0048.

Jarvis, N.J., 2007. A review of non-equilibrium water flow and solute transport in soil macropores: principles, controlling factors and consequences for water quality. Eur. J. Soil Sci. 58, 523–546. https://doi.org/10.1111/j.1365-2389.2007.00915.x.

Javaux, M., Schröder, T., Vanderborght, J., Vereecken, H., 2008. Use of a three-dimensional detailed modeling approach for predicting root water uptake. Vadose Zone J. 7, 1079–1088. https://doi.org/10.2136/vzj2007.0115.

Kroes, J.G., Van Dam, J.C., Bartholomeus, R.P., Groenendijk, P., Heinen, M., Hendriks, R.F.A., Mulder, H.M., Supit, I., Van Walsum, P.E.V., 2017. SWAP Version 4: Theory and Description of User Manual. Wageningen Environmental Research, Wageningen Report 2780.

Lobsey, C.R., Rossel, R.A.V., 2016. Sensing of soil bulk density for more accurate carbon account. Eur. J. Soil Sci. 67, 504–513. https://doi.org/10.1111/ejss.12355.

Luo, X., Wells, L.G., 1992. Evaluation of gamma ray attenuation for measuring soil bulk density Part I. Laboratory investigation. Am. Soc. Agric. Eng. 35, 17–26. https://doi.org/10.13031/2013.28564.

Minasny, B., McBratney, A.B., 2018. Limited effect of organic matter on soil available water capacity. Eur. J. Soil Sci. 69, 39–47. https://doi.org/10.1111/ejss.12475.

Mualem, Y., 1976. A new model for predicting the hydraulic conductivity of unsaturated porous media. Water Resour. Res. 12, 513–522. https://doi.org/10.1029/WR012i003p00513.

Oliveira, J.C.M., Appoloni, C.R., Coimbra, M.M., Reichardt, K., Bacchi, O.O.S., Ferraz, E., Silva, S.C., Galvão Filho, W., 1998. Soil structure evaluated by gamma-ray attenuation. Soil Tillage Res. 48, 127–133. https://doi.org/10.1016/S0167-1987(98)00130-5.

Pachepsky, Y., Rawls, W.J., Gimenez, D., 2001. Comparison of soil water retention at field and laboratory scales. Soil Sci. Soc. Am. J. 65, 460–462. https://doi.org/10.2136/sssaj2001.652460x.

Peters, A., 2013. Simple consistent models for water retention and hydraulic conductivity in the complete moisture range. Water Resour. Res. 49, 6765–6780. https://doi.org/10.1002/wrcr.20548.

Peters, A., Durner, W., 2008. Simplified evaporation method for determining soil hydraulic properties. J. Hydrol. 356, 147–162. https://doi.org/10.1016/j.jhydrol.2008.04.016.

Peters, A., Iden, S.C., Durner, W., 2015. Revisiting the simplified evaporation method: identification of hydraulic functions considering vapor, film and corner flow. J. Hydrol. 527, 531–542. https://doi.org/10.1016/j.jhydrol.2015.05.020.

Pinheiro, E.A.R., De Jong van Lier, Q., Metselaar, K., 2018. A matric flux potential approach to assess plant water availability in two climate zones in Brazil. Vadose Zone J. 17, 160083. https://doi.org/10.2136/vzj2016.09.0083.

Pires, L.F., Bacchi, O.O.S., Reichardt, K., 2005. Soil water retention curve determined by gamma-ray beam attenuation. Soil Tillage Res. 82, 89–97. https://doi.org/10.1016/j.still.2004.06.003.

Raats, P.A.C., 1977. Laterally confined, steady flows of water from sources and to sinks in unsaturated soils. Soil Sci. Soc. Am. J. 41, 294–304. https://doi.org/10.2136/sssaj1977.03615995004100020025x.

Ritter, A., Hupet, F., Munoz-Carpena, R., Lambot, S., Vanclooster, M., 2003. Using inverse methods for estimating soil hydraulic properties from field data as an alternative to direct methods. Agric. Water Manage. 59, 76–96. https://doi.org/10.1016/S0378-3774(02)00160-9.

Roy, D., Jia, X., Steele, D.D., Lin, D., 2018. Development and comparison of soil water release curves for three soils in the red river valley. Soil Sci. Soc. Am. J. 82, 568–577. https://doi.org/10.2136/sssaj2017.09.0324.

Schaap, M.G., Leij, F.J., 2000. Improved prediction of unsaturated hydraulic conductivity with the Mualem-van Genuchten model. Soil Sci. Soc. Am. J. 64, 843–851. https://doi.org/10.2136/sssaj2000.643843x.

Schaap, M.G., Leij, F.J., Van Genuchten, M.Th., 2001. ROSETTA: a computer program for estimating soil hydraulic parameters with hierarchical pedotransfer functions. J. Hydrol. 251, 163–176. https://doi.org/10.1016/S0022-1694(01)00466-8.

Schindler, U., 1980. Ein Schnellverfahren zur Messung der Wasserleitfähigkeit im teilgesättigten Boden an Stechzylinderproben. Arch. Acker-u. Pflanzenbau u. Bodenkd. 24, 1–7.

Shi, J., Li, S., Zuo, Q., Ben-Gal, A., 2015. An index for plant water deficit based on root-weighted soil water content. J. Hydrol. 522, 285–294. https://doi.org/10.1016/j.jhydrol.2014.12.045.

Siltecho, S., Hammecker, C., Sriboonlue, V., Clermont-Dauphin, C., Trelo-ges, V., Antonino, A.C.D., Angulo-Jaramillo, R., 2015. Use of field and laboratory methods for estimating unsaturated hydraulic properties under different land uses. Hydrol. Earth Syst. Sci. 19, 1193–1207. https://doi.org/10.5194/hess-19-1193-2015.

Šimůnek, J., Wendroth, O., Van Genuchten, M.Th., 1998. Parameter estimation analysis of the evaporation method for determining soil hydraulic properties. Soil Sci. Soc. Am. J. 62, 894–905. https://doi.org/10.2136/sssaj1998.03615995006200040007x.

Šimůnek, J., van Genuchten, M.Th., Šejna, M., 2016. Recent developments and applications of the HYDRUS computer software packages. Vadose Zone J. https://doi.org/10.2136/vzj2016.04.0033.

Sinclair, T.R., Ludlow, M.M., 1986. Influence of soil water supply on the plant water balance of four tropical grain legumes. Aust. J. Plant Physiol. 13, 329–341. https://doi.org/10.1071/PP9860329.

Sinclair, T.R., Holbrook, N.M., Zwieniecki, M.A., 2005. Daily transpiration rates of woody species on drying soils. Tree Physiol. 25, 1469–1472. https://doi.org/10.1093/treephys/25.11.1469.

Solone, R., Bittelli, M., Tomei, F., Morari, F., 2012. Errors in water retention curves determined with pressure plates: effects on the soil water balance. J. Hydrol. 470-471, 65–74. https://doi.org/10.1016/j.jhydrol.2012.08.017.

Taylor, S.A., Ashcroft, G.M., 1972. Physical Edaphology. Freeman and Co. San Francisco, California, pp. 434–435.

Twarakavi, N.K.C., Sakai, M., Šimůnek, J., 2009. An objective analysis of the dynamic nature of field capacity. Water Resour. Res. 45, W10410. https://doi.org/10.1029/2009WR007944.

Van Dam, J.C., Stricker, J.N.M., Droogers, P., 1994. Inverse method to determine soil hydraulic functions from multistep outflow experiments. Soil Sci. Soc. Am. J. 58, 647–652. https://doi.org/10.2136/sssaj1994.03615995005800030002x.

Van Genuchten, M.Th., 1980. A closed-form equation for predicting the hydraulic conductivity of unsaturated soils. Soil Sci. Soc. Am. J. 44, 892–898. https://doi.org/10.2136/sssaj1980.03615995004400050002x.

Van Genuchten, M.Th., Leij, F.J., Yates, S.R., 1991. The RETC Code for Quantifying the Hydraulic Functions of Unsaturated Soils, Version 1.0. EPA Report 600/2-91/065. U.S. Salinity Laboratory, USDA, ARS, Riverside, California.

Vereecken, H., Huisman, J.A., Bogena, H., Vanderborght, J., Vrugt, J.A., Hopmans, J.W., 2008. On the value of soil moisture measurements in vadose zone hydrology: a

review. Water Resour. Res. 44, W00D06. https://doi.org/10.1029/2008WR006829.
Vereecken, H., Weynants, M., Javaux, M., Pachepsky, Y., Schaap, M.G., Van Genuchten, M.Th., 2010. Using pedotransfer functions to estimate the van Genuchten-Mualem soil hydraulic properties: a review. Vadose Zone J. 9https://doi.org/10.2136/vzj2010.0045. 975-820.
Vogel, M.M., Orth, R., Cheruy, F., Hagemann, S., Lorenz, R., Van der Hurk, B.J.J.M., Seneviratne, S.I., 2017. Regional amplification of projected changes in extreme temperatures strongly controlled by soil-moisture temperature feedbacks. Geophys. Res. Lett. 44, 1511–1519. https://doi.org/10.1002/2016GL071235.
Wang, C.H., Willis, D.L., Loveland, W.D., 1975. Characteristics of ionizing radiation. In: Wang, C.H., Willis, D.L., Loveland, W.D. (Eds.), Radiotracer Methodology in the Biological Environmental, and Physics Sciences. Prentice-Hall, Englewood Cliffs, NJ, pp. 39–74.
Wang, L., D`Odorico, P., Evans, J.P., Eldridge, D.J., McCabe, M.F., Caylor, K.K., King, E.G., 2012. Dryland ecohydrology and climate change: critical issues and technical advances. Hydrol. Earth Syst. Sci. 16, 2585–2603. https://doi.org/10.5194/hess-16-2585-2012.
Wendroth, O., Ehlers, W., Hopmans, J.W., Kage, H., Halbertsma, J., Wösten, J.H.M., 1993. Reevaluation of the evaporation method for determining hydraulic functions in unsaturated soils. Soil Sci. Soc. Am. J. 57, 1436–1443. https://doi.org/10.2136/sssaj1993.03615995005700060007x.
Weynants, M., Vereecken, H., Javaux, M., 2009. Revisiting Vereecken pedotransfer functions: introducing a closed-form hydraulic model. Vadose Zone J. 8, 86–95. https://doi.org/10.2136/vzj2008.0062.
Wind, G.P., 1968. Capillary conductivity data estimated by a simple method. In: In: Rijtema, P.E., Wassink, H. (Eds.), Water in the Unsaturated Zone. Proc. Wageningen Symp. June 1966, vol. 1. IASAH, Gentbrugge, Belgium, pp. 181–191.
Zuo, Q., Shi, J., Li, Y., Zhang, R., 2006. Root length density and water uptake distributions of winter wheat under sub-irrigation. Plant Soil 285, 45–55. https://doi.org/10.1007/s11104-005-4827-2.